A Parametric Study of Bubble Cloud Dynamics near a Wall in an Acoustic Field

Chao-Tsung Hsiao*; Jingsen Ma; Georges L. Chahine

DYNAFLOW, INC., Jessup, MD, USA

Abstract

A parametric study is conducted to investigate bubble cloud dynamics near a rigid wall when excited by a sinusoidal pressure field. It is shown that a preferred driving frequency which can incur the strongest collective bubble behavior and result in the highest pressure impact on the nearby wall exists for a given bubble cloud initial condition. Such preferred driving frequency is strongly dependent on the driving amplitude but independent on the initial ambient pressure. The preferred driving frequency decrease as the driving amplitude is increased and approaches the natural frequency of bubble cloud predicted by linear theory when the driving amplitude is very small.

Keywords: Cloud Cavitation, Bubble Dynamics, Multiphase Flow

Introduction

The collapse of a cloud of microbubbles near a rigid boundary is known to be as one of the most destructive forms of cavitation due collective bubble dynamics resulting in high pressure generation during successive collapses and rebounds. Cloud cavitation can be observed in hydrodynamic applications such as on rotating propellers or hydrofoils[1]–[5] as well as in high intensity acoustic fields such as in ultrasonic devices, Shock Wave Lithotripsy (SWL) for kidney stone fragmentation [6] and High Intensity Focused Ultrasound (HIFU) for tumor ablation [7]. Our previous studies [3], [4] have shown that the bubbles in the cloud, collapse in a cascading fashion with the bubbles farthest from the wall and cloud center collapsing first and those closest to the wall and center collapsing last. This results in a pressure wave moving inward and toward the wall. In order to contribute to the understanding of the physics involved in the complex interaction between the many bubbles and the imposed pressure field, and to predict the loading on a nearby object, we have applied our coupled Eulerian-Lagrangian two-phase flow modeling [8], [9] to an initially spherical bubble cloud to study the effects of the excitation amplitude and frequency. The advantage of the Eulerian-Lagrangian numerical approach is that it is a multiscale approach and captures key characteristics of both the bubbles' dynamics and the overall cloud dynamics. It also enables one to account for the often-neglected slip velocity between the bubbles and the liquid, which results in micro-streaming with the bubbles migrating significantly when the driving pressure amplitude is increased. In [9] we also considered the effects of the initial bubble radii, the bubble distribution, and the cloud distance from the wall and found that the strongest collective bubble behavior occurs at a preferred driving frequency for a given initial cloud condition. At this preferred driving frequency, pressure peaks orders of magnitudes higher than the excitation pressure, result from bubble interaction. However, our previous studies mainly focused on a high ambient pressure. In this study we will study the effect of the ambient pressure on the bubble cloud dynamics. In addition, the driving pressure amplitude and frequency are varied for different ambient pressures to investigate their effects on the bubble cloud dynamics and the resulting pressure at the wall as the bubble cloud collapses.

Numerical Method

The two-phase mixture in the bubble cloud is treated as a continuum with the continuity and momentum equations expressed as follows:

$$\frac{\partial \rho_m}{\partial t} + \nabla \cdot \left(\rho_m \mathbf{u} \right) = 0, \qquad \rho_m \frac{D\mathbf{u}}{Dt} = -\nabla p + \mu_m \nabla^2 \mathbf{u}, \tag{1}$$

where ρ_m, μ_m, $\mathbf{u}$, and p are respectively the mixture density, dynamic viscosity, velocity, and pressure. ρ_m and μ_m are related to the liquid and gas properties and to the gas volume fraction, α, by:

$$\rho_m = (1-\alpha)\rho_l + \alpha\rho_g, \qquad \mu_m = (1-\alpha)\mu_l + \alpha\mu_g. \tag{2}$$

Eq. (1) is coupled with equations describing the dynamics of the discrete individual bubbles in the cloud. Knowing at each instant all bubble radii and locations provides α (thus ρ_m and μ_m) as a function of space and time and substitutes for the need of a mixture equation of state to close the system of equations. Each bubble is treated as a source, which represents volume change, and a dipole to represent translation. For each bubble, the equivalent

*Corresponding Author, Chao-Tsung Hsiao: ctsung@dynaflow-inc.com

spherical radius, $R(t)$, is obtained using a modified Keller-Herring equation [5], which accounts for the mixture compressibility and non-uniform pressure field:

$$\left(1-\frac{\dot{R}}{c_m}\right)R\ddot{R}+\frac{3}{2}\left(1-\frac{\dot{R}}{3c_m}\right)\dot{R}^2=\frac{\mathbf{u}_s^2}{4}+\frac{1}{\rho_m}\left(1+\frac{\dot{R}}{c_m}+\frac{R}{c_m}\frac{d}{dt}\right)\left[p_v+p_g-p_{enc}-\frac{2\gamma}{R}-4\mu_m\frac{\dot{R}}{R}\right], \quad (3)$$

where c_m is the local sound speed in the mixture, p_v is the liquid vapor pressure, p_g is the bubble gas pressure, and γ is the surface tension. The term $\mathbf{u}_s^2/4$, accounts for the pressure resulting from the slip velocity, $\mathbf{u}_s=\mathbf{u}_{enc}-\mathbf{u}_b$, between the host medium velocity, $\mathbf{u}_{enc}$, and the bubble velocity, $\mathbf{u}_b$, with [6]. p_{enc} and $\mathbf{u}_{enc}$ are the encountered pressures and velocities averaged over the bubble surface to account for local non-uniform flow. The bubble trajectory is obtained using the following equation of motion [7]:

$$\frac{d\mathbf{u}_b}{dt}=\left(\frac{\rho_l}{\rho_g}\right)\left[\frac{3}{8R}C_D\,|\mathbf{u}_s|\,\mathbf{u}_s+\frac{1}{2}\left(\frac{d\mathbf{u}_{enc}}{dt}-\frac{d\mathbf{u}_b}{dt}\right)-\frac{\nabla p}{\rho_l}+\frac{(\rho_b-\rho_l)}{\rho_l}g+\frac{3C_L}{4\pi}\frac{\sqrt{\nu}}{R}\frac{\mathbf{u}_s\times\boldsymbol{\Omega}}{\sqrt{|\boldsymbol{\Omega}|}}+\frac{3\dot{R}}{2R}\mathbf{u}_s\right], \quad (4)$$

where C_L is a lift coefficient, $\boldsymbol{\omega}$ is the local vorticity, and C_D is a drag coefficient. The last term is the Bjerknes force due to coupling between bubble volume rate and bubble motion.

Numerical Simulations and Discussion

We consider an initially spherical bubble cloud with a radius, A_0, (Fig. 1), driven by a sinusoidal pressure, $P(t)=P_0\left[1-\xi\sin(2\pi f t)\right]$, where P_0 is the initial and average ambient pressure, $\xi=P_{amp}/P_0$ is the normalized pressure oscillation amplitude, and f is the frequency. The cloud center is initially at a distance X_0 from a rigid wall and is composed of small bubbles of initial radii R_0. The bubbles are randomly distributed within A_0, resulting in a quasi-uniform initial α_0 within the cloud and all bubbles are initially at equilibrium with the pressure P_0. We can identify in this problem two groups of parameters: one for the imposed pressure field (driving pressure and frequency) and one for the bubble cloud characteristics (cloud and bubble sizes and the void fraction).

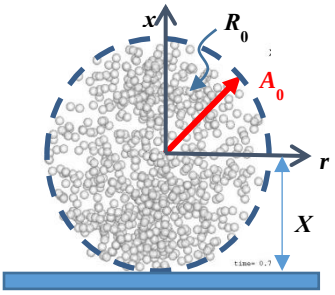

Fig. 1: Schematic of the problem of the dynamics of a bubble cloud near a rigid wall.

Fig. 2 shows an example time sequence of the bubble cloud response during the first cycle of oscillation for $A_0=X_0$=1.5 mm, R_0=50 μm, and α_0=5%, driven by the imposed pressure P_0 = 1 atm, ζ= 0.9 and f = 7kHz. The color contours indicate the pressure inside each bubble and the corresponding pressure loading at the wall. It is seen that the bubbles in the cloud grow first then collapse in a cascading fashion starting with the bubbles at the cloud top (farthest from the wall) collapsing first, and finally those on the bottom (closest to the wall) collapsing last and resulting a high pressure loading at the wall.

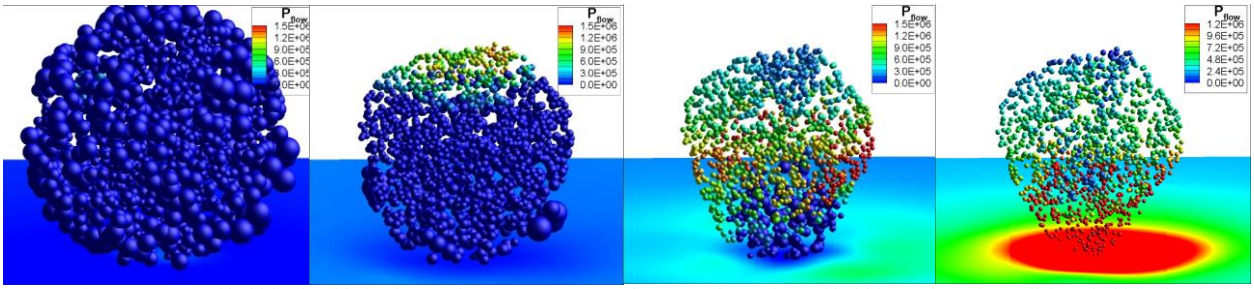

Fig. 2: Time sequence of bubble cloud behaviors and pressure contours shown on the surface of bubbles and nearby wall for a bubble cloud with the initial conditions, R_0=50 μm, α_0=5%, and $A_0=X_0$=1.5 mm, driven by a sinusoidal pressure field with P_0=1 atm, ζ=0.9, and f=7 kHz.

Our previous studies [8], [9] have shown that for a given bubble cloud initial geometric condition, the pressure loading at the wall when the bubble cloud collapses is highly dependent on the driving pressure amplitude and frequency. A preferred driving frequency was found to result in a maximum pressure loading for a given ζ. However, the previous studies focused on a high initial pressure, P_0 = 10 atm, and thus it would be interesting to investigate if the same trend exists for different initial pressures.

To start with, Fig. 3 compares the effect of the driving frequency on the pressure loading at the wall centre when P_0 = 1 atm (which is a more practical case for ultrasonic applications than the previously studied P_0 = 10 atm) and ζ=0.9. It is seen that the highest collective effects appear here close to 7 kHz. This is compared with the results of

*Corresponding Author, Chao-Tsung Hsiao: ctsung@dynaflow-inc.com

P_0 = 10 atm as shown in Fig. 4. It can be seen that only a small shift in the peak driving frequency (7 kHz vs. 8 kHz) can be observed between these two initial ambient pressures even though the resulting maximum collapse pressure is more than five times higher for P_0 = 10 atm. This implies that the preferred driving frequency may be little dependent on the initial ambient pressure. We are considering next a larger range of pressure changes to understand this behaviour.

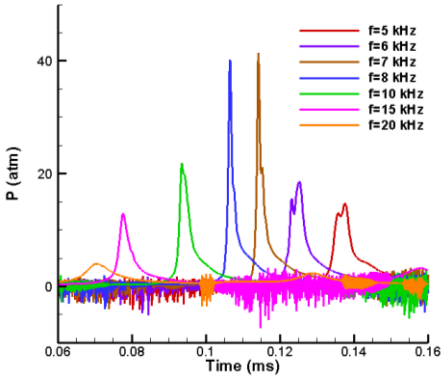

Fig. 3: Pressure versus time at the wall center created by bubble clouds for different driving frequency for P_0=1 atm, ζ=0.9, R_0=50μm, α_0=5%, and A_0=X_0=1.5 mm.

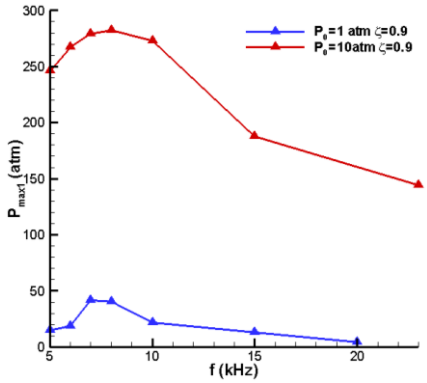

Fig. 4: Effect of initial ambient pressure on P_{max1} vs f, for ζ=0.9, R_0=50μm, α_0=5%, and A_0=X_0=1.5 mm.

Fig. 5 shows for the same driving frequency, f = 8 kHz, how the peak pressure, P_{max1}, varies with P_0 . It is seen that the maximum pressure loading at the wall increases as the initial ambient pressure is increased indicating stronger bubble collapses at the higher pressures. This, however, reaches a plateau at the largest initial ambient pressures considered.

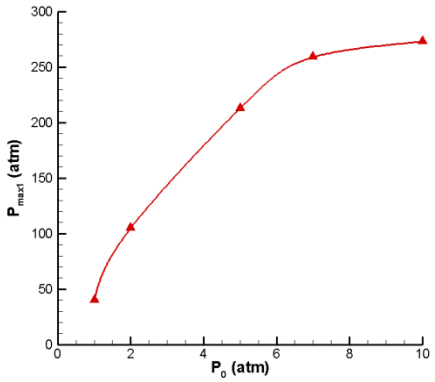

Fig. 5: Effect of initial ambient pressure on the maximum pressure loading at the wall center for f=8kHz, ζ=0.9, R_0=50μm, α_0=5%, and A_0=X_0=1.5 mm

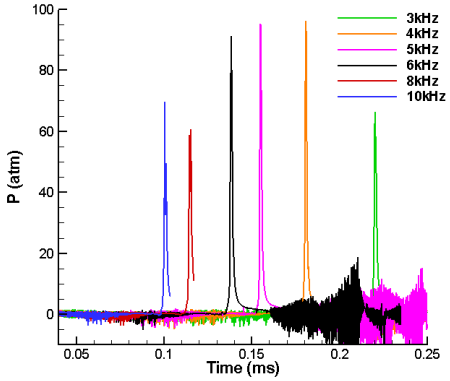

Fig. 6: Pressure versus time at the wall center created by bubble clouds for different driving frequency for P_0=1 atm, ζ=1.25, R_0=50μm, α_0=5%, and A_0=X_0=1.5 mm.

Another set of cases at P_0 = 1 atm and ζ=1.25 is simulated and compared to ζ=0.9 for different acoustic driving frequencies, to examine the effect of the driving amplitude, ζ, on the peak amplitude at the wall. It is seen from Fig. 7 that the preferred driving frequency, f_{max} , is about 4 kHz for ζ=1.25, while it was 8 kHz for ζ=0.9. This indicates a strong influence of ζ. The effects of the driving amplitude on P_{max1} vs f is also seen in Fig. 7 It can be seen that the peak value of the pressure at the wall, P_{max1}, increases and f_{max} decreases as ζ is increased. It is important to note that the preferred driving frequency, f_{max}, highlighted here is different from the natural frequency of a bubble cloud derived from linear bubble dynamics theory by [10]:

$$f_{cloud} = f_0\left(1+\frac{12}{\pi^2}\frac{A_0^2}{R_0^2}\frac{\alpha_0}{1-\alpha_0}\right)^{-1/2} \quad \text{with} \quad f_0 = \frac{1}{2\pi}\sqrt{\frac{P_{g0}}{\rho R_0^2}\left(3-\frac{2\gamma}{P_{g0}R_0}\right)}, \tag{5}$$

which gives a value of f_{cloud} = 23 kHz for the current case. Further expanding the range of ζ will allow one to investigate such dependency. Fig. 8 shows the dependency of f_{max} on ζ. It can be seen that when ζ is less than 0.2, f_{max} is compatible with f_{cloud}. For ζ > 0.2, f_{max} deviates significantly from f_{cloud}. f_{max} decreases almost linearly with

*Corresponding Author, Chao-Tsung Hsiao: ctsung@dynaflow-inc.com

increasing ξ until ξ >1 where the f_{max} seems to reach a plateau. A plausible explanation for this saturation is the appearance of inertial cavitation for ξ >1 ,where the bubble expansion and collapse are controlled by inertia of the fluid [11].

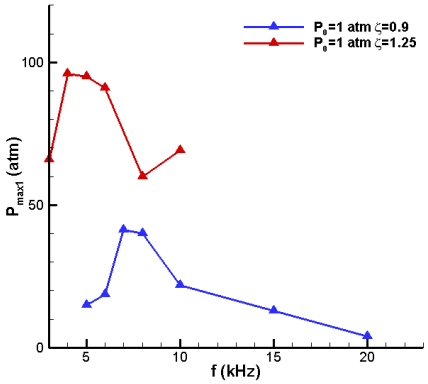

Fig. 7: Effect of driving pressure amplitude on P_{max1} vs f, for P_0=1 atm, R_0=50μm, α_0=5%, and A_0=X_0=1.5 mm

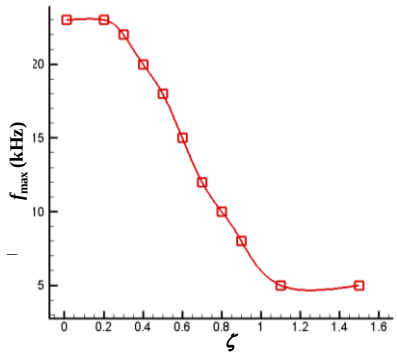

Fig. 8: driving frequency, for different relative driving pressure amplitudes, b) bubble cloud resonance frequency versus ξ, for P_0=1 atm, R_0=50μm, α_0=5%, and A_0=X_0=1.5 mm.

Conclusions

The dynamics of a bubble cloud subjected to a sinusoidal pressure field near a rigid wall is numerically studied using an Eulerian/Lagrangian two-phase flow model. Very strong pressures are generated at the wall during the cloud collapse at a resonance driving frequency. The study shows that the magnitude of pressure at the wall highly depends on the ambient pressure but not the resonance frequency. The study also shows that both the magnitude of the pressure and the resonance frequency are strongly dependent on the amplitude of the driving pressure. The magnitude of the pressure increases as the driving pressure is increased. The resonance frequency decreases as the driving amplitude is increased and approaches the natural frequency of the bubble cloud at small amplitude oscillations.

Acknowledgements

This work was funded by ONR under Contract No. N00014-15-C-5029 monitored by Dr. Ki-Han Kim.

References

[1] L. van Wijngaarden, "On the collective collapse of a large number of cavitation bubbles in water," in *11th Int. Congr. of Appl. Mech*, 1964.

[2] I. Hansson, V. Kedrinskii, and K. Mørch, "On the dynamics of cavity clusters," *J. Phys. D. Appl. Phys.*, vol. 15, no. 9, p. 1725, 1982.

[3] G. L. Chahine, "Cloud Cavitation: Theory," in *Proceedings of the 14th Symposium on Naval Hydrodynamics; Ann Arbor Michigan National Academy*, 1983, pp. 165–195.

[4] G. L. Chahine and R. Duraiswami, "Dynamical Interactions ina Multi-Bubble Cloud," *ASME J. Fluids Eng.*, vol. 114, no. 4, pp. 680–686, 1992.

[5] G. L. Chahine, C.-. T. Hsiao, and R. Raju, "Scaling of Cavitation Bubble Cloud Dynamics on Propellers," in *Advanced Experimental and Numerical Techniques for Cavitation Erosion Prediction*, vol. 160, K.-H. Kim, G. L. Chahine, J.-P. Franc, and A. Karimi, Eds. Spinger, Berlin, 2014, pp. 345–373.

[6] E. A. Brujan, T. Ikeda, K. Yoshinaka, and Y. Matsumoto, "The final stage of the collapse of a cloud of bubbles close to a rigid boundary," *Ultrason. Sonochem.*, vol. 18, no. 1, pp. 59–64, 2011.

[7] B. C. Tran, T. L. Hall, J. B. Fowlkes, and C. A. Cain, "Microbubble-enhanced cavitation for noninvasive ultrasound surgery," *IEEE Trans. Ultrason. Ferroelectr. Freq. Control*, vol. 50, no. 10, pp. 1296–1304, Oct. 2003.

[8] J. Ma, C.-T. Hsiao, and G. L. Chahine, "Euler-Lagrange Simulations of Bubble Cloud Dynamics Near a Wall," *ASME J. Fluids Eng.*, vol. 137, no. 4, pp. 041301–10, 2015.

[9] J. Ma, C.-T. Hsiao, and G. L. Chahine, "Numerical Study of Bubble Cloud Dynamics near a Rigid Wall," *Ultrason. Sonochemisty*, vol. 40, pp. 944–954, 2018.

[10] C. E. E. Brennen, *Cavitation and bubble dynamics*, vol. 9, no. 1. New York: Oxford University Press, 1995.

[11] T. J. Matula, "Inertial cavitation and single-bubble sonoluminescence," *Philos. Trans. R. Soc. A Math. Phys. Eng. Sci.*, vol. 357, no. 1751, pp. 225–249, 1999.

*Corresponding Author, Chao-Tsung Hsiao: ctsung@dynaflow-inc.com